

# The supergiant optical counterpart of ULX P13 in NGC7793\*

C. Motch<sup>1,\*\*</sup>, M.W. Pakull<sup>1</sup>, F. Grisé<sup>2</sup>, and R. Soria<sup>3</sup>

<sup>1</sup> CNRS, Université de Strasbourg, Observatoire Astronomique, 11 rue de l'Université, F-67000 Strasbourg, France

<sup>2</sup> Department of Physics and Astronomy, University of Iowa, Van Allen Hall, Iowa City, IA 52242, USA

<sup>3</sup> Mullard Space Science Laboratory, University College London, Holmbury St Mary, Surrey RH5 6NT, UK

Received , accepted

**Key words** X-rays: binaries - black hole physics

We have identified the optical counterpart of the ULX source P13 in the nearby spiral galaxy NGC 7793. The object is a  $V \sim 20.5$  mag star, ten times brighter than any other established counterpart of a ULX in nearby galaxies. Medium resolution optical spectroscopy carried out in 2008 and 2009 with the ESO-VLT reveals the presence of narrow high order Balmer, HeI and MgII absorption lines indicating a late B type supergiant companion star with mass between 10 and 20  $M_{\odot}$ . Stellar H $\beta$  and HeII  $\lambda 4686$  emission lines are also seen superposed on the photospheric spectrum. We detect different patterns of radial velocity variations from the emission and absorption lines over a time interval of one month. The velocity of the high order Balmer absorption lines changes by  $\sim 100 \text{ km s}^{-1}$  while the H $\beta$  and HeII  $\lambda 4686$  emission components vary by about the same amount but with a different phasing. Assuming that the observed velocity changes trace the motion of the mass-donor star and of the X-ray source implies a mass of the accreting black hole in the range of 3 to 100  $M_{\odot}$  with a most probable value of  $\sim 10$  to 20  $M_{\odot}$ . We expect an orbital period in the range of 20 to 40 days based on the low density of the supergiant star. P13 is likely in a short-lived, and thus rare high X-ray luminosity evolutionary state associated with the ascension of the donor star onto the supergiant stage.

© 2010 WILEY-VCH Verlag GmbH & Co. KGaA, Weinheim

## 1 The ULX P13 in NGC 7793

Many galaxies harbour non-nuclear X-ray sources with  $L_X$  higher than  $10^{39}$  and up to several  $10^{40} \text{ erg s}^{-1}$ , generally known as ultraluminous X-ray sources (ULXs). X-ray variability shows that the majority are accreting compact objects. If the Eddington limit is not violated, or if no strong radiation beaming occurs, such isotropic luminosities imply compact stellar masses up to a few 100  $M_{\odot}$ . However, presently available stellar evolutionary models at solar metallicity do not predict compact remnants that massive. Even intermediate-mass black holes with  $M \sim 10^3 M_{\odot}$  have been suggested, based on X-ray spectral and timing arguments (see e.g. Miller et al. 2004). Determining black hole masses is therefore a key issue for understanding the X-ray emission mechanism and the evolutionary status of ULXs.

NGC 7793 is an Sd galaxy member of the Sculptor Group of galaxies located at a distance of 3.9 Mpc (Karachentsev et al. 2003). *ROSAT* PSPC observations (Read & Pietsch 1999) have revealed that its X-ray emission is dominated by a single source, P13, located at the southern edge of the galaxy and exhibiting evidence of variability over a 5 month time interval. *Chandra* revisited NGC 7793 in 2003 for 49 ks (Pannuti et al. 2006), providing an accurate source position at RA = 23:57:51.01, Dec = -32:37:26.62 (J2000) with a formal 90% confidence radius of 0.4". A simple power law

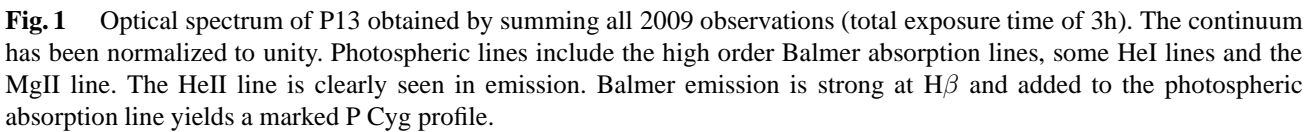
does not fit well the *Chandra* ACIS-S spectrum ( $\chi^2 = 201$  for 181 dof). However, the addition of a soft or of a hot blackbody decreases the  $\chi^2$  to acceptable values ( $\chi^2 \sim 185$  for 179 dof in both cases). The corresponding two best fits are  $\Gamma = 1.10 \pm 0.06$ ,  $kT = 0.18 \pm 0.03 \text{ keV}$  and  $\Gamma = 2.14 \pm 0.28$ ,  $kT = 1.72 \pm 0.13 \text{ keV}$ . With  $L_X \sim 4 \times 10^{39} \text{ erg s}^{-1}$ , P13 is a bona fide ULX. A blue  $V \sim 20.5$  stellar object falls right in the middle of the small *Chandra* error circle, leaving no doubt about the identification of P13 counterpart, the brightest ULX optical counterpart presently known (Pakull et al. 2010, in prep).

## 2 Optical properties

In 2008 and 2009 we obtained ESO-VLT observations with the aim of deriving the spectral type of the companion star and of measuring the dynamical masses of the binary components. Unfortunately, very few of the scheduled observations were eventually executed in 2008 and 2009. Additional runs are expected to be carried out in 2010. On 2008 November 23 and 27, two 40 min long spectra were obtained with FORS1 and the 600B Grism providing a spectral resolution of  $\sim 600$  over the wavelength range 3500–6000 Å. The five 2009 40 min long exposures were obtained with a higher resolution of  $\sim 1600$  over the 3700–5200 Å range using FORS2 and grism 1200B. Observations took place on November 17 and December 9, 11, 13 and 14. The rectified sum of all optical spectra obtained in 2009 shown in Fig. 1 reveals many deep unresolved Balmer and HeI absorption

\* Based on optical observations obtained at ESO under programme 084.D.0881(A)

\*\* Corresponding author: e-mail: christian.motch@unistra.fr



### 3 Radial velocities

Fig. 1 shows high order Balmer lines mostly in absorption, whereas emission components become conspicuous at  $H\gamma$  and below. Using a cross-correlation method we monitored the velocity of the 5 Balmer lines contained in the 3750 to 3900Å interval. We tested several different templates: a) the straight average of all spectra with and without velocity correction, b) a B8I spectrum extracted from the Walborn & Fitzpatrick (1990) atlas and c) a TLUTSY B-STAR06 model (Lanz & Hubeny 2007) with  $T_{\text{eff}} = 15,000$  K and  $\log g = 2.0$ , degraded to the FORS2 resolution. Results are not sensitive to the actual template used or to the inclusion of additional absorption lines at slightly longer wavelengths such as Ca H&K,  $H\epsilon$  and  $H\delta$ . Errors on velocities were derived from sub-exposures measurements and estimated to be of the order of  $7 \text{ km s}^{-1}$ .

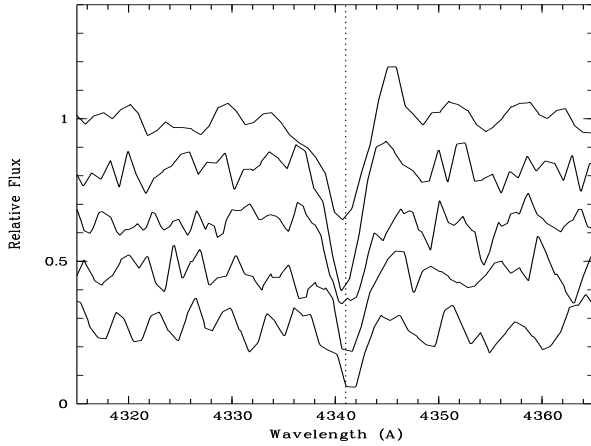


**Fig. 2** Variation of the  $H\gamma$  absorption line profile with time. Spectra have been shifted in flux for clarity. From top to bottom, Nov. 17, Dec. 9, 11, 13 and 14.

In order to monitor the behaviour of Balmer emission components, we subtracted from the observed spectra a template photospheric spectrum shifted at the measured velocity of the high order Balmer absorption lines. We tested again two of the templates considered for the cross-correlation method, namely the Walborn & Fitzpatrick (1990) atlas spectrum and the TLUTSY model without finding noticeable effects on the results. The subtracted spectra only display emissions at  $H\gamma$  and  $H\beta$ . The centroid of the  $H\beta$  emission line was measured by fitting a Gaussian profile. Unfortunately, the  $H\gamma$  emission is too weak to provide useful velocity information. The  $\text{HeII } \lambda 4686$  line has a broad resolved profile on the top of which a narrower component appears on occasion. Since the line does not overlap with any strong photospheric feature, we directly measured its position on the original spectra by fitting Gaussian profiles to the broad or narrow components or using a cross-correlation method. Again, all approaches gave quite similar results.

We find that the velocity of the absorption features changes by  $105.5 \pm 13 \text{ km s}^{-1}$  over the 27 day time interval between the first and last observation. The velocity shift is also visible in the  $H\gamma$  line plotted in Fig. 2, although this particular line is clearly contaminated by residual emission.

Most of the velocity change of the  $H\beta$  emission line occurs between the first and second data points separated by 22 days (see Fig. 3) with a total amplitude of  $73.4 \pm 11.0 \text{ km s}^{-1}$ . A PCyg profile is patent in several spectra. However, the line equivalent width (EW) remains stable at a value of  $\sim -3.5 \text{ \AA}$ . In contrast, the  $\text{HeII } \lambda 4686$  line exhibits larger profile and velocity variations (see Fig. 4). Ignoring the second observation in which the line was particularly broad and weak, the total velocity amplitude of the  $\text{HeII}$  line is  $104 \pm 15 \text{ km s}^{-1}$ , i.e. comparable to that of the Balmer absorption lines. The line EW varies from  $-1$  to  $-2.4 \text{ \AA}$ .

The radial velocity curves plotted in Fig. 5 show a rather complex pattern which is hard to interpret considering the scarcity of the available data. One can remark, however, that

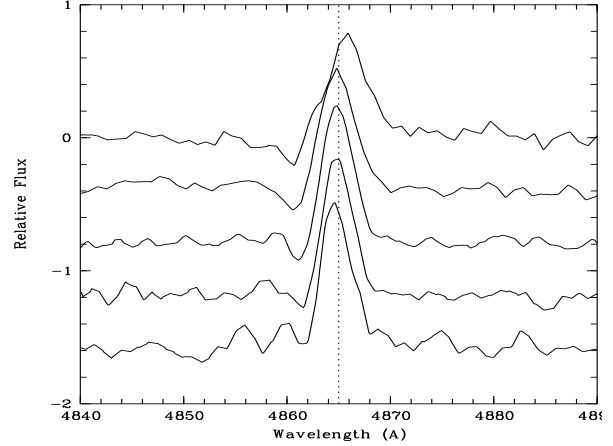


**Fig. 3** Variation of the  $H\beta$  emission line profile with time. A TLUTSY/BSTAR06 model spectrum shifted at the velocity of the high order Balmer absorption lines was subtracted from the observed spectrum. Spectra are shifted in intensity for clarity. From top to bottom, Nov. 17, Dec. 9, 11, 13 and 14.

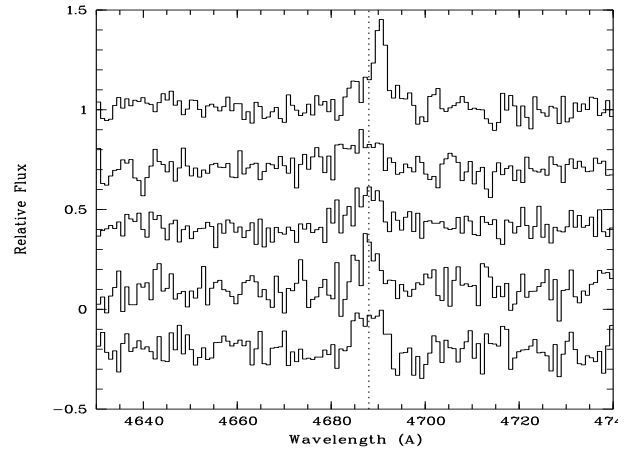


**Fig. 4** Variation of the  $\text{HeII } \lambda 4686$  emission line profile with time. Spectra are shifted in intensity for clarity. From top to bottom, Nov. 17, Dec. 9, 11, 13 and 14.

between the single November 17 observation and the mean of the December observations, the velocities of the emission and absorption components roughly varied in opposite directions. Such a behaviour would be expected in a double line spectroscopic binary. The velocity of the absorption lines probably reflects to a large extent the orbital motion of the mass-donor star. Unfortunately, its smooth variation during the 4 day long run in December is not accompanied by any correlated change in the  $H\beta$  or  $\text{HeII}$  line velocities. This hints at an orbital phasing different from  $180^\circ$  between absorption and emission lines, or worse, at a mostly random variation. P13 might thus be not as clean as one would have liked to measure dynamical masses of both components. It is fairly possible that none of the emission lines accurately follows the motion of the compact object, neither in amplitude nor in phase. Many supergiant stars ex-

hibit Balmer emission lines with PCyg profiles produced in massive winds. In the case of P13, the difference in velocity between the peak emission and absorption is  $\sim 250$ – $330 \text{ km s}^{-1}$ , fully consistent with the escape velocity from a  $20 M_{\odot}$  star having a  $60 R_{\odot}$  radius. Therefore, emission from an X-ray photoionized stellar wind could well add to the light originating from the accretion disc and considerably alter the  $H\beta$  radial velocity curve.

Similar considerations apply to the HeII line. Its velocity profile might include emissions from the X-ray heated companion hemisphere or from various structures of the accretion disc. In fact, previous optical spectroscopic observations of ULXs cast some doubt on the reliability of the HeII  $\lambda 4686$  line as a tracer of the motion of the accreting component (Roberts et al. 2010). Most ULXs are likely to undergo noticeable X-ray heating effects with an irradiated to unirradiated optical flux ratio closer to that seen in galactic low-mass X-ray binaries than shown by classical high-mass X-ray binaries (HMXRBs) (Copperwheat et al. 2005; Grisé et al. 2008). This could imply, for instance, that the HeII  $\lambda 4686$  line does not follow the velocity of the accreting component but rather that of the disc bulge at the point where the stream of matter escaping L1 impacts the edge of the disc (see e.g. Pearson et al. 2006). Moreover, although for the first time in a ULX we detect photospheric absorption lines, in other ULXs spectral signatures from the companion stars have not yet been found (Roberts et al. 2010).

However, in the case of P13, the roughly opposite velocity variations of the HeII +  $H\beta$  and high order Balmer absorption lines suggest that these lines may still be used to constrain to some extent the dynamical parameters. In addition, the moderately high  $L_X/L_{\text{bol}}$  of  $\sim 6$  is similar to that of the X-ray luminous HMXRB LMC X-4 in which the HeII  $\lambda 4686$  line does trace the motion of the neutron star ( $K_X \sim K_{\text{HeII}}$ ; Kelley et al. 1983).

Adopting the Roche lobe overflow formalism of Eggleton (1983) yields orbital periods of about 20 to 40 days for a large range of mass ratios and for stellar radii between 40 and  $60 R_{\odot}$ . The fact that the total velocity amplitudes of Balmer absorption and HeII lines are both larger than  $\sim 100 \text{ km s}^{-1}$  implies a mass ratio  $q = M_{\text{opt}}/M_X$  in the range of 0.2 to 3.2. Values of  $K_X \sim K_{\text{opt}} \sim 50 \text{ km s}^{-1}$  are reached for  $i \sim 30^\circ$ . A mass ratio close to 1 is supported by the nearly equal amplitude of the absorption and emission lines radial velocity curves and therefore hints at a black hole mass of  $\sim 10$ – $20 M_{\odot}$ . Taken at face value, our observations do not support the presence of an intermediate mass black hole in P13.

## 4 Discussion and Conclusions

Determining whether ULXs harbour stellar mass or in some cases intermediate mass black holes can only be settled by measuring orbital periods and dynamical masses. However, the optical faintness of most ULXs is a challenge for medium resolution spectroscopic monitoring, even using 8m-

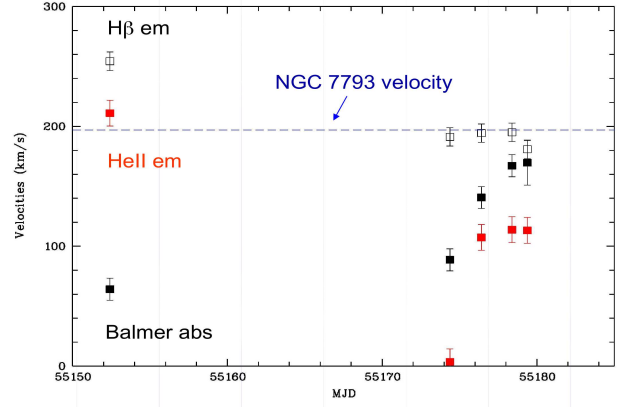


**Fig. 5** Radial velocity curves of the high order Balmer absorption lines (black filled squares) of the  $H\beta$  emission (open squares) and of the He  $\lambda 4686$  emission line (red filled squares). The horizontal line shows the velocity of the nearby interstellar gas.

class telescopes. P13 is the first ULX in which optical spectral signatures of the mass-donor star are detected. These lines provide both a reliable indication of the spectral type and luminosity class of the companion star and at the same time means to measure accurate orbital velocities. The high optical luminosity and the late B spectral type of the companion star clearly demonstrate that the star has left the main sequence and is now rapidly evolving towards a red supergiant. This evolutionary stage corresponds to the most X-ray luminous phases of any ULX (Rappaport et al. 2005) and should last no more than  $\sim 10^6$  years and may be as short as a few  $10^4$  years (Patruno & Zampieri 2008). In comparison, the life time of ULXs in which the mass-donor star is a sub-giant is much longer ( $\sim 10^7$  years). Population models indeed confirm that systems like P13 are rare and should account for only  $\sim 5\%$  of all ULXs (Rappaport et al. 2005).

## References

- Copperwheat, C., Cropper, M., Soria, R., & Wu, K. 2005, *MNRAS*, 362, 79
- Eggleton, P. P. 1983, *ApJ*, 268, 368
- Grisé, F., Pakull, M. W., Soria, R., et al. 2008, *A&A*, 486, 151
- Karachentsev, I. D., Grebel, E. K., Sharina, M. E., et al. 2003, *A&A*, 404, 93
- Kelley, R. L., Jernigan, J. G., Levine, A., Petro, L. D., & Rappaport, S. 1983, *ApJ*, 264, 568
- Lanz, T. & Hubeny, I. 2007, *ApJS*, 169, 83
- Markova, N. & Puls, J. 2008, *A&A*, 478, 823
- Meynet, G. & Maeder, A. 2000, *A&A*, 361, 101
- Miller, J. M., Fabian, A. C., & Miller, M. C. 2004, *ApJ*, 614, L117
- Pannuti, T. G., Schlegel, E. M., & Lacey, C. K. 2006, in *IAU Symp.*, Vol. 230, *Populations of High Energy Sources in Galaxies*, ed. E. J. A. Meurs & G. Fabbiano, 197–198

- Patruno, A. & Zampieri, L. 2008, MNRAS , 386, 543  
Pearson, K. J., Hynes, R. I., Steeghs, D., et al. 2006, ApJ , 648, 1169  
Rappaport, S. A., Podsiadlowski, P., & Pfahl, E. 2005, MNRAS , 356, 401  
Read, A. M. & Pietsch, W. 1999, A&A, 341, 8  
Roberts, T., Gladstone, J., Goulding, A., et al. 2010, AN , these proceedings  
Walborn, N. R. & Fitzpatrick, E. L. 1990, PASP , 102, 379